Electronic Supplementary Material (ESI) for Sensors & Diagnostics.

Rapid and simultaneous detection of SARS-CoV-2 and influenza A using vertical flow assay based on AAO and SERS nanotags

Yu Lu[a,b,c], Ruihua Fei[a,b,c], Jiahe Zhang[a,b,c], Geng Zhu[a,b,c], Xiufang Mo[a,b,c], Yu Wan[a, d], Yan Huang[a,b,c], Qingjiang Sun[a], Dianhuai Meng[e,*], Xiangwei Zhao[a,b,c,*]

a, State Key Laboratory of Bioelectronics, School of Biological Science and Medical Engineering, Southeast University, Nanjing 210096, China. E-mail: xwzhao@seu.edu.cn

b, Institute of Biomaterials and Medical Devices, Southeast University, Suzhou 215163, China

c, Southeast University Shenzhen Research Institute, Shenzhen 518000, China

d, Jiangsu Simcere Pharmaceutical Co., Ltd, Nanjing 210042, China

e, Rehabilitation Medical Center, The First Affiliated Hospital of Nanjing Medical University, Nanjing, 210029, China. Email: dhdream@126.com

SI-1 Enhancement factor (EF) calculation

The SERS enhancement factor (EF) of Au@Ag@Au was evaluated by

$$EF = \frac{I_{SERS}}{I_{bulk}} * \frac{N_{bulk}}{N_{SERS}}$$

Where I_{SERS} and I_{bulk} were intensities of the same band of SERS spectrum and normal Raman spectrum, respectively. N_{SERS} and N_{bulk} were the number of molecules participating in SERS signal and Raman signal, respectively. In our experiment, laser-illuminated area, laser power, exposure time and microscope magnification were the

same. The droplet volume was the same, and the number of NBA molecules was proportional to its concentration. Therefore, EF was roughly estimated by

$$EF = \frac{I_{SERS}}{I_{bulk}} * \frac{C_{bulk}}{C_{SERS}}$$

Where I_{SERS} and I_{bulk} were intensities of NBA of 591 cm^{-1} of SERS spectrum and normal Raman spectrum, respectively. C_{SERS} and C_{bulk} were concentrations of NBA participating in SERS signal and Raman signal, respectively. The UV-Vis spectra of NBA before and after adsorbed to Au@Ag were measured in Figure S1(a) to calculate the concentration of NBA in Au@Ag@Au NPs. As shown in Figure S1(b), the SERS intensities of NBA from Au@Ag@Au NPs and Si substrate were 38980 and 2166, respectively. The concentrations of NBA were 1.69×10^{-6} M and 10 mM, respectively. Thus, the EF of Au@Ag@Au was estimated to be 1.06×10^{5}.

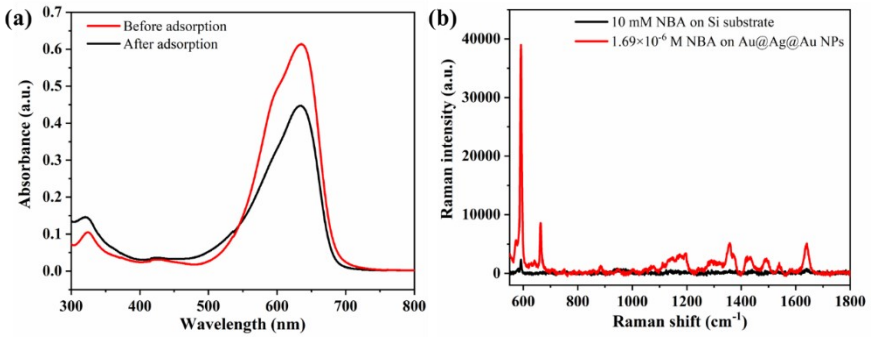

Figure S1 (a) Absorption spectra of NBA before and after adsorbed to Au@Ag (b) Raman spectra of NBA on different substrates: 10 mM NBA on Si substrate (black line), and 1.69×10^{-6} M NBA on Au@Ag@Au NPs (red line).

Figure S2 (a) Absorption spectra and (b) SERS spectra of $Au@Ag^{NBA}@Au$ NPs with different volumes of Au^{I} solution.

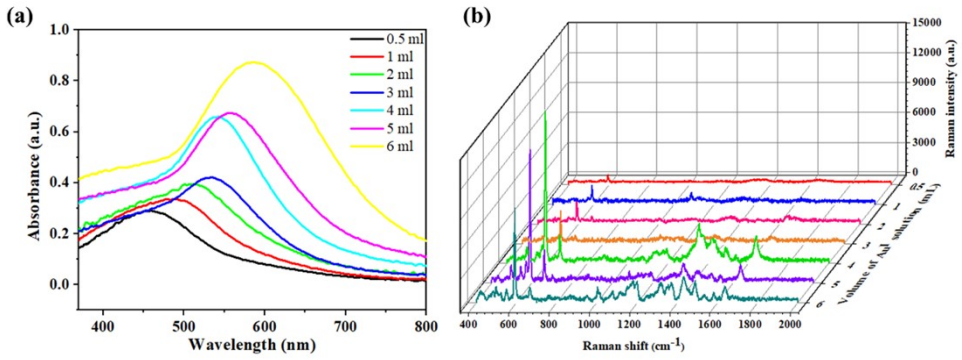

Figure S3 Zeta potentials of nanoparticles

The negative zeta potential of Au NPs arises from citrate ligand. Meanwhile, the positive zeta potentials of residual NPs arise from CTAC which is a cationic surfactant.

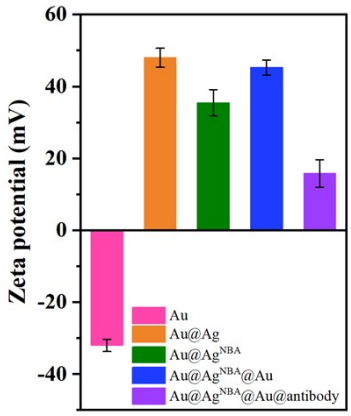

Figure S4 (a) Element mapping image of Au@Ag NPs (b) Element mapping image of Au@Ag@Au NPs (c) 2D Z-normal refractive index monitor in numerical simulation of Au@Ag@Au NPs.

Figure S4(a) and Figure S4(b) show the element mapping image of Au@Ag and Au@Ag@Au NPs, respectively. The structure parameters of Au@Ag@Au NPs were configurated according to element mappings in TEM images. The diameters of Au core and Au@Ag NPs were 15 nm and 56 nm, respectively. The thickness of outer Au shell was 11 nm and there was a 1 nm gap between Au@Ag and outer Au shell. The dielectric

functions of Au and Ag were taken from Johnson and Christy. The wavelength of excitation source was 785 nm and the mesh size was 0.1 nm. Figure S4(c) shown the result from 2D Z-normal refractive index monitor.

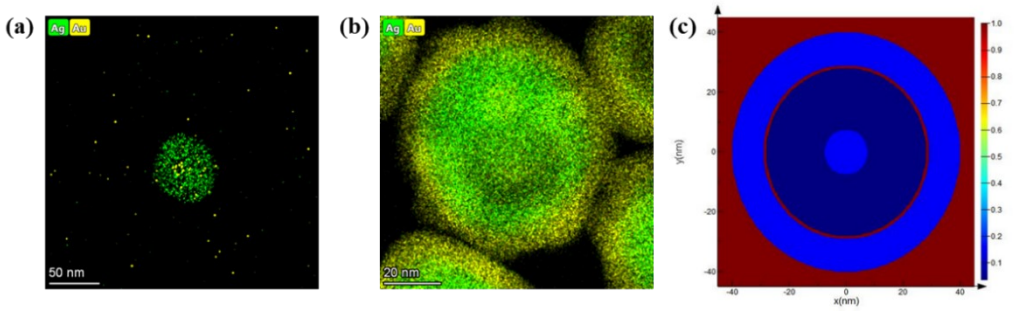

Figure S5 Modification steps of AAO

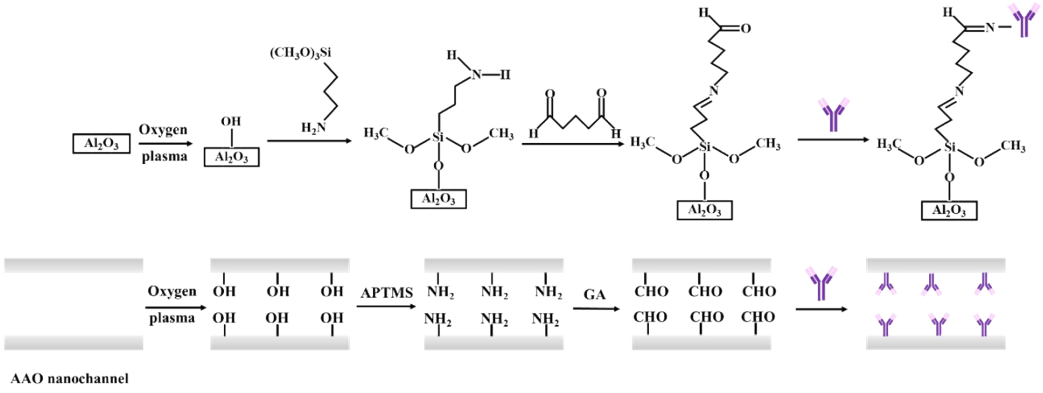

Figure S6 Depth mapping of test spot at 10 ng/ml of SARS-CoV-2 NP

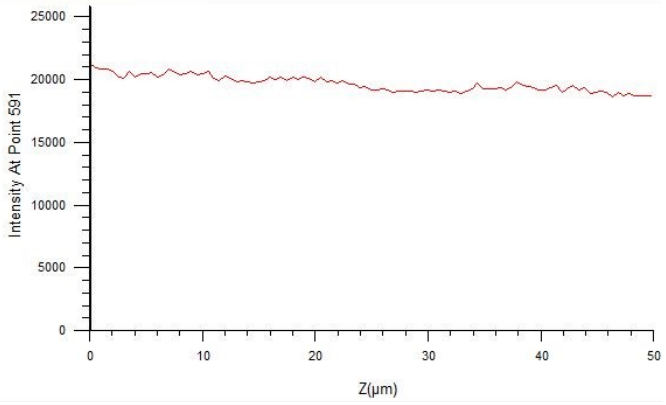

Figure S7 Colorimetric results of SARS-CoV-2 and influenza A measured by commercial LFA strips. (a) Assay results of SARS-CoV-2 NP in the range of 0-100 ng/ml (b) Assay results of influenza A antigen in the range of 0-100 ng/ml.

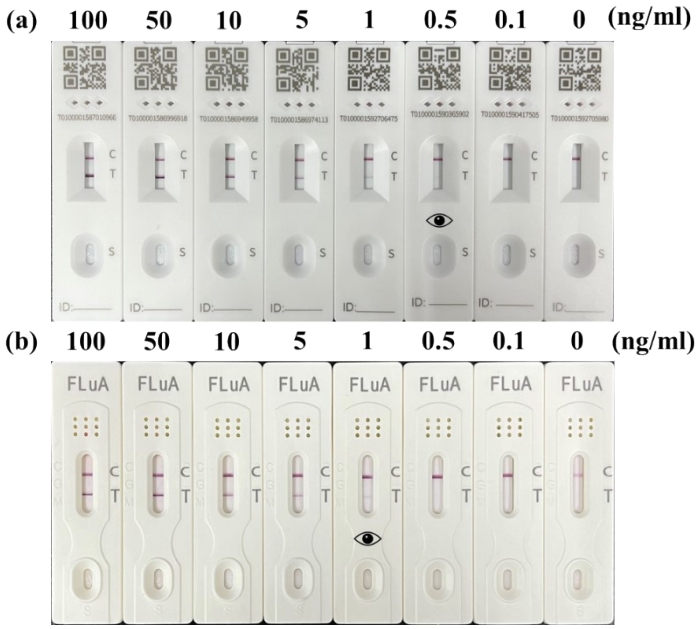

Figure S8 SERS intensities at 591 cm^{-1} and 1621 cm^{-1} of 1 ng/ml SARS-CoV-2 NP and Influenza A antigen collected from 15 substrates

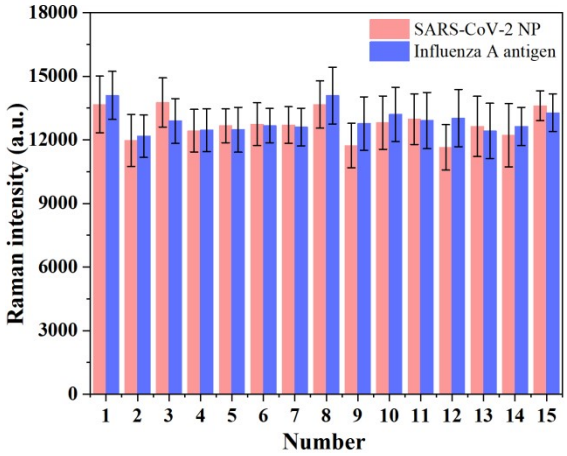

Figure S9 Images of commercial LFA strips of three repeated detections at three concentrations of SARS-CoV-2 NP (100 ng/ml, 10 ng/ml and 1 ng/ml)

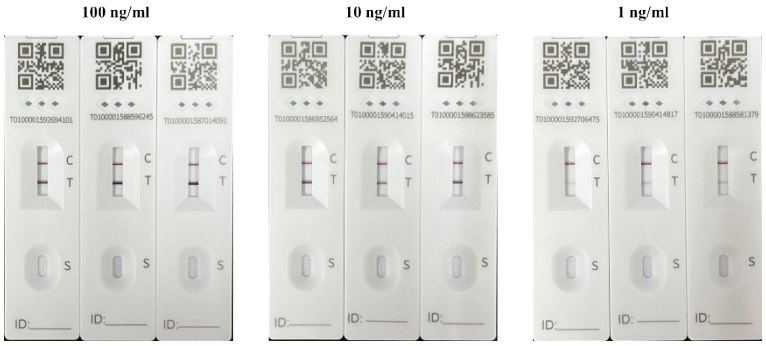

Figure S10 SERS intensities at 591 cm^{-1} of 1 μg/ml SARS-CoV-2 NP after SERS-VFA device being exposed in the air for 8 weeks

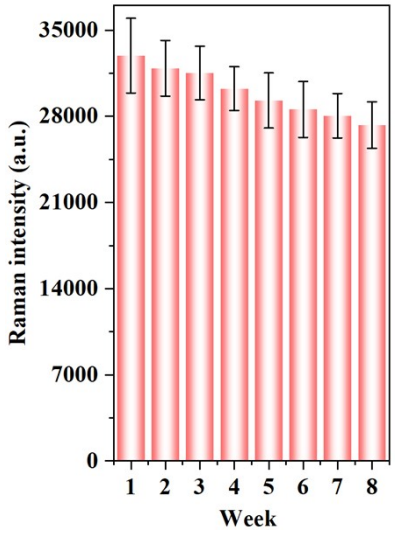

Figure S11 (a) SERS spectra of Au@Ag^{NBA}@Au SERS nanotags mixed with complex samples (10 mM PBS, 50 mM Tris-HCl, saliva, sputum and nasal mucus). (b) SERS intensities at 591 cm^{-1} of Au@Ag^{NBA}@Au SERS nanotags mixed with complex samples (10 mM PBS, 50 mM Tris-HCl, saliva, sputum and nasal mucus). Inset is the appearance of six Au@Ag^{NBA}@Au SERS nanotags mixed with complex samples: 10 mM PBS, 50 mM Tris-HCl, saliva, sputum and nasal mucus, respectively.

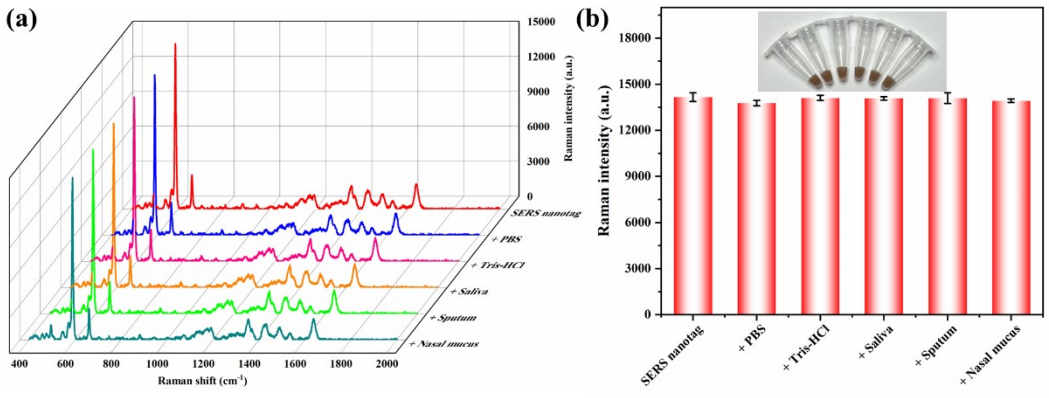

Figure S12 (a) SERS spectrum of negative sputum sample (b) Image of AAO after negative sputum sample detection (c) Image of absorption pad after negative sputum sample detection

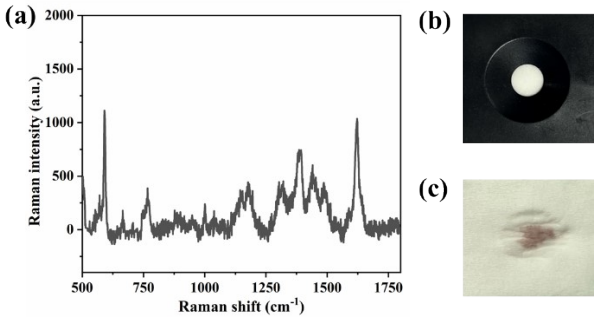

Table S1 Concentrations of SARS-CoV-2 NP and Influenza A antigen in ten samples in the cross-reactivity test.

Sample Number	SARS-CoV-2 NP (ng/ml)	Influenza A antigen (ng/ml)
1	0.02	0.2
2	0.1	0.2
3	0.5	0.2
4	2	0.2
5	16	0.2

6	0.5	0.02
7	0.5	0.2
8	0.5	0.85
9	0.5	3
10	0.5	30

Table S2 Comparison of the proposed SERS-VFA with other immunoassays for simultaneous detection of SARS-CoV-2 and influenza A

Method	Analytes	Dynamic range	LOD	Test time
SERS-LFA [1]	SARS-CoV-2 virus	50-1000 PFU/mL	5.2 PFU/mL	Not mentioned
	Influenza A virus	168-8064 HAU/mL	23 HAU/mL	
SERS-LFA [2]	SARS-CoV-2 S protein	0.01-100 ng/ml	8 pg/ml	30 min
	H1N1	10^2-10^7 copy/ml	85 copies/ml	
Fluorescence-LFA [3]	SARS-CoV-2 N protein	0.01-100 ng/ml	50 pg/ml	15 min
	Flu A H1NI viron	100-10^5 pfu/ml	50 pfu/ml	
Fluorescence-LFA [4]	SARS-CoV-2 N protein	10-500 pg/mL	8 pg/mL	15 min
	Influenza A virus	500-10000 copies/mL	488 copies/mL	
Electrochemical immunoassay [5]	SARS-CoV-2 S protein	0.15-100 ng/ml	150 pg/ml	>105 min

	H1N1 HA	4-64 unit/ml	1.12 unit/ml	
SERS aptasensor [6]	SARS-CoV-2 virus	0-5000 PFU/ml	0.78 PFU/ml	15 min
	Influenza A virus	0-2016 HAU/ml	0.62 HAU/ml	
Magnetic particle based LFA [7]	SARS-CoV-2 N protein	0-50 ng/ml	0.0086 ng/mL	20 min
	Flu A N protein	0-50 ng/ml	0.012 ng/mL	
PLGA nanovesicles based immunoassay [8]	SARS-CoV-2 S protein	10^{-5}-10^{-12} g/ml	143 fg/ml	>2 h
	Influenza A virus	10-10^{6} fg/ml	32.37 fg/ml	
SERS-VFA This work	SARS-CoV-2 N protein	0.01 ng/ml-1 μg/ml	0.47 pg/ml	15 min
	Influenza A antigen	0.01 ng/ml-1 μg/ml	0.62 pg/ml	

Reference

[1] M.D. Lu, Y. Joung, C.S. Jeon, S. Kim, D. Yong, H. Jang, S.H. Pyun, T. Kang and J. Choo, Dual-mode SERS-based lateral flow assay strips for simultaneous diagnosis of SARS-CoV-2 and influenza a virus, Nano Converg., 2022, 9, 39.

[2] Z.Z. Liu, C.W. Wang, S. Zheng, X.S. Yang, H. Han, Y.W. Dai and R. Xiao, Simultaneously ultrasensitive and quantitative detection of influenza A virus, SARS-CoV-2, and respiratory syncytial virus via multichannel magnetic SERS-based lateral flow immunoassay, Nanomedicine, 2023, 47, 102624.

[3] C.W. Wang, X.S. Yang, S. Zheng, X.D. Cheng, R. Xiao, Q.J. Li, W.Q. Wang, X.X. Liu and S.Q. Wang, Development of an ultrasensitive fluorescent immunochromatographic assay based on multilayer quantum dot nanobead for simultaneous detection of SARS-CoV-2 antigen and influenza A virus, Sensor Actuat. B Chem., 2021, 345, 130372.

[4] W.Q. Wang, X.S. Yang, Z. Rong, Z.J. Tu, X.C. Zhang, B. Gu, C.W. Wang and S.Q. Wang, Introduction of graphene oxide-supported multilayer-quantum dots nanofilm into multiplex lateral flow immunoassay: A rapid and ultrasensitive point-of-care testing technique for multiple respiratory viruses, Nano Res., 2023, 16, 3063-3073.

[5] J.Y Li, R. Lin, Y. Yang, R.T. Zhao, S.P. Song, Y. Zhou, J.Y. Shi, L.H. Wang, H.B. Song and R.Z. Hao, Multichannel Immunosensor Platform for the Rapid Detection of SARS-CoV-2 and Influenza A(H1N1) Virus, ACS Appl. Mater. Interfaces, 2021, 13, 22262-22270.

[6] H. Chen, S.K. Park, Y. Joung, T. Kang, M.K. Lee and J. Choo, SERS-based dual-mode DNA aptasensors for rapid classification of SARS-CoV-2 and influenza A/H1N1 infection, Sensor Actuat. B Chem., 2022, 355, 131324.

[7] G. Liu, Q. Zhang, K. Wang, J.Q. Niu, A. Gao, M.R. Chen, Z.Y. Yang, C. Zhou, G. Gao, D.X. Cui, Multiplex and Ultrasensitive Detection of Severe Acute Respiratory Syndrome Coronavirus 2 and Influenza A/B Nucleocapsid Proteins Based on Nanometer-Sized Core–Shell Superparamagnetic Antifouling Probes, ACS Appl. Nano Mater., 2023, 6, 5, 3344-3356.

[8] I.M. Khoris, A.B. Ganganboina, T. Suzuki, E.Y. Park, Self-assembled chromogen-loaded polymeric cocoon for respiratory virus detection, Nanoscale, 2021, 13, 388-396.